# Practical identifiability of the manipulator link stiffness parameters

Alexandr Klimchik, Stéphane Caro, Anatol Pashkevich

ASME 2013 International Mechanical Engineering Congress & Exposition
IMECE2013
November 15-21, 2013, San Diego, CA, USA

IMECE2013-63123

# PRACTICAL IDENTIFIABILITY OF THE MANIPULATOR LINK STIFFNESS PARAMETERS

**Alexandr Klimchik[a,b], Stéphane Caro[b], Anatol Pashkevich[a,b],**
[a]Ecole des Mines de Nantes, 4 rue Alfred-Kastler, 44307 Nantes, France
[b]Institut de Recherches en Communications et Cybernétique de Nantes, UMR CNRS 6597, France

## ABSTRACT

The paper addresses a problem of the manipulator stiffness modeling, which is extremely important for the precise manufacturing of contemporary aeronautic materials where the machining force causes significant compliance errors in the robot end-effector position. The main contributions are in the area of the elastostatic parameters identification. Particular attention is paid to the practical identifiability of the model parameters, which completely differs from the theoretical one that relies on the rank of the observation matrix only, without taking into account essential differences in the model parameter magnitudes and the measurement noise impact. This problem is relatively new in robotics and essentially differs from that arising in geometrical calibration. To solve the problem, several physical and statistical model reduction methods are proposed. They are based on the stiffness matrix sparseness taking into account the physical properties of the manipulator elements and also on the heuristic selection of the practically non-identifiable parameters that employs numerical analyses of the parameter estimates. The advantages of the developed approach are illustrated by an application example that deals with the stiffness modeling of an industrial robot used in aerospace industry.

## KEYWORDS

Robotic machining, stiffness modeling, elastostatic identification, parameter identifiability

## 1. INTRODUCTION

Application area of industrial robots is continuously increasing, they become more and more popular in many technological processes, including precise high-speed machining. For this process, the robot is subject to essential external loadings caused by the machining force that may lead to non-negligible end-effector deflections [1]. This feature becomes extremely important in the aerospace industry, where the accuracy requirements are very high but the materials are hard to process. In this case, the manipulator stiffness modeling and corresponding error compensation technique are the key issues [2-5].

In the manipulator stiffness modeling, there are three main approaches that can be summarized as follows: the Finite Element Analysis (FEA), the Matrix Structural Analysis (MSA), and the Virtual Joint Method (VJM). The most accurate of them is the FEA-based technique [6], which allows presenting manipulator components with their true shape and dimension. However, this method is usually applied at the final design stage because of the high computational expenses [7]. The MSA method [8] incorporates the main ideas of the FEA, but operates with rather large elements – 3D flexible beams. This obviously leads to the reduction of the computational efforts, but does not eliminate the disadvantages of FEA. And finally, the VJM method [9-13], is based on the extension of the traditional rigid model by adding the virtual joints (localized springs), which describe the elastic deformations of the links, joints and actuators. This technique provides reasonable trade-off between the model accuracy and computational complexity, which will be further used in this paper. However, evaluation or identification of the stiffness model parameters is not a trivial problem.

The main difficulty here is that the straightforward application of the VJM method yields very high number of parameters that differ in their magnitudes and in their impact on the model precision. Moreover, direct application of this technique may produce redundant models that are not suitable for calibration. In particular, attempts to solve the identification problem for the whole set of the elastostatic parameters (258 for 6 d.o.f. manipulator) leads to the fail of the numerical routines that is caused by singularity of the relevant observation matrix. It is worth mentioning that similar problem is also known in geometric calibration where the concept of complete-irreducible-continues model has been introduced and relevant algebraic tools for the model reduction have been developed [14-16]. However, in elastostatic calibration there is an additional difficulty caused by high number of relatively small parameters for which the measurement noise impact is very essential. As follows from our experience, the identification results may violate fundamental physical properties of the stiffness matrices, such as positive-definiteness and symmetry, and are not acceptable for the compliance error compensation (more details are given in Section 3.2 presenting a motivation example). For this reason, this paper introduces a new notion of practical identifiability and proposes corresponding model reduction methods that allow obtaining reliable results in real industrial environment.

To address the above mentioned problem, the remainder of the paper is organized as follows. Section 2 presents the stiffness modeling background. Section 3 describes the calibration procedure and contains the motivation example allowing us to define the research problems. In Section 4, the developed model reduction methods are presented. Section 5 contains an application example and illustrates advantages of the proposed technique. And finally, Section 6 summarizes the main contributions of the paper.

## 2. STIFFNESS MODELING BACKGROUND

Let us consider elastostatic model of a general serial manipulator, which consists of a fixed “Base”, a serial chain of flexible “Links”, a number of flexible actuated joints “Ac” and an “End-effector” (Fig. 1). It is assumed that all links are separated by either rotational or translational joints. Such architecture can be found most of industrial serial robots.

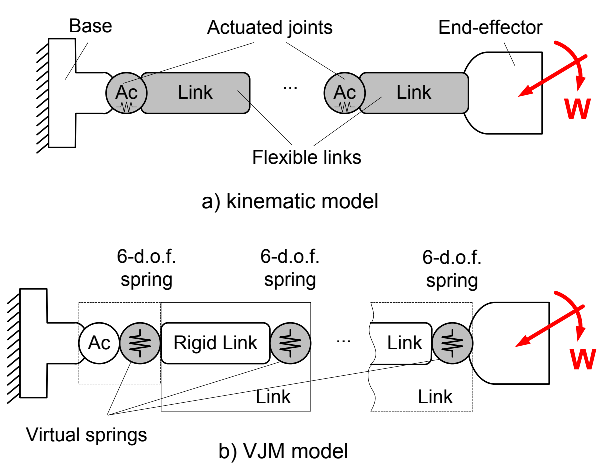


**Figure 1** Serial manipulator and its VJM model

In order to evaluate the stiffness of the considered manipulator, let us apply the virtual joint method (VJM), which is based on the lump modeling approach [12]. According to this approach, the original rigid model should be extended by adding virtual joints (localized springs), which describe elastic deformations of the links. Besides, virtual springs are included in the actuated joints, in order to take into account the stiffness of the control loop. Under these assumptions, the kinematic chain can be described by the following serial structure:

(a) a rigid link between the manipulator base and the first actuated joint described by the constant homogenous transformation matrix $\mathbf{T}_{\text{Base}}$;

(b) several flexible actuated joints described by the homogeneous matrix function $\mathbf{T}^{i}_{\text{Joint}}(q^{i}+\theta^{i}_{\text{Ac}})$, which depends on the actuated joint variable $q^{i}$ and the virtual joint variable $\theta^{i}_{\text{Ac}}$ that takes into account the joint compliance;

(c) a set of rigid links, which are described by the constant homogenous transformation matrices $\mathbf{T}^{i}_{\text{Link}}$;

(d) a set of 6-d.o.f. virtual joints that take into account the link flexibility and are described by the homogeneous matrix function $\mathbf{T}_{\text{VJM}}(\boldsymbol{\theta}^{i}_{\text{Link}})$ which depends on the virtual joint variables $\boldsymbol{\theta}^{i}_{\text{Link}}=(\theta^{i}_{\text{x}},\theta^{i}_{\text{y}},\theta^{i}_{\text{z}},\theta^{i}_{\varphi\text{x}},\theta^{i}_{\varphi\text{y}},\theta^{i}_{\varphi\text{z}})$ corresponding to the translation/rotation deflections in/around the axis x, y, z;

(e) a rigid link from the last joint to the end-effector, described by the constant homogenous matrix transformation $\mathbf{T}_{\text{Tool}}$.

In the frame of these notations, the final expression defining the end-effector location subject to variations of all joint coordinates may be presented as the product of the following homogenous matrices and matrix functions

$$\mathbf{T}=\mathbf{T}_{\text{Base}}\cdot\left[\prod_{i=1}^{n}\mathbf{T}^{i}_{\text{Joint}}(q^{i}+\theta^{i}_{\text{Ac}})\cdot\mathbf{T}^{i}_{\text{Link}}\cdot\mathbf{T}_{\text{VJM}}\left(\boldsymbol{\theta}^{i}_{\text{Link}}\right)\right]\cdot\mathbf{T}_{\text{Tool}} \tag{1}$$

where $n$ is the number of links/joints, and the components $\mathbf{T}_{\text{Base}}$, , $\mathbf{T}^{i}_{\text{Joint}}(.)$, $\mathbf{T}^{i}_{\text{Link}}$, $\mathbf{T}_{\text{VJM}}(.)$, $\mathbf{T}_{\text{Tool}}$ may be factorized with respect to the terms including the joint variables (in order to simplify computing of the derivatives). For further convenience, after extraction from the homogeneous matrix $\mathbf{T}$ rotation and translation components [17], the kinematic model can be rewritten in more conventional form

$$\mathbf{t}=\mathbf{g}(\mathbf{q},\boldsymbol{\theta}) \tag{2}$$

where $\mathbf{g}(.)$ denotes relevant vector function, the vector $\mathbf{t}=(\mathbf{p},\boldsymbol{\varphi})^{\text{T}}$ defines the end-effector position $\mathbf{p}=(x,y,z)^{\text{T}}$ and orientation $\boldsymbol{\varphi}=(\varphi_{\text{x}},\varphi_{\text{y}},\varphi_{\text{z}})^{\text{T}}$, the vector $\mathbf{q}=(q_{1},q_{2},...,q_{\text{n}})^{\text{T}}$ aggregates all actuated coordinates, the vector $\boldsymbol{\theta}=(\theta_{1},\theta_{2},...,\theta_{n\theta})^{\text{T}}$ collects all virtual joint coordinates, and $n_{\theta}$ is the number of the virtual joints. It should be noted that here the values of coordinates $\mathbf{q}$ are completely defined by the robot controller, while the values of the virtual joint coordinates

$\boldsymbol{\theta}$ depend on the external loading applied to the robot end-effector.

To take into account manipulator stiffness properties, let us assume that variations in the virtual joint variables $\boldsymbol{\theta}$ generate the force/torque applied to the corresponding links that are evaluated by the following linear equation (it can be treated as a generalised Hooke's law for the manipulator) $\boldsymbol{\tau}_\theta = \mathbf{K}_\theta \cdot \boldsymbol{\theta}$, where $\boldsymbol{\tau}_\theta = (\tau_{\theta,1},\, \tau_{\theta,2},\, ...,\, \tau_{\theta,n\theta})^{\mathrm{T}}$ is the aggregated vector of the virtual joint reactions, $\mathbf{K}_\theta = diag(\mathbf{K}_{\theta,1},\, \mathbf{K}_{\theta,2},\, ...,\, \mathbf{K}_{\theta,n\theta})$ is the aggregated virtual spring stiffness matrix, and $\mathbf{K}_{\theta,i}$ is the spring stiffness matrix of the corresponding link/joint. Further, let us apply the principle of virtual work assuming that the joints are given small, arbitrary virtual displacements $\Delta\boldsymbol{\theta}$ in the equilibrium neighborhood. Then, the virtual work of the external wrench $\mathbf{W}$ applied to the end-effector along the corresponding displacement $\Delta\mathbf{t} = \mathbf{J}_\theta \cdot \Delta\boldsymbol{\theta}$ is equal to $(\mathbf{W}^{\mathrm{T}} \cdot \mathbf{J}_\theta) \cdot \Delta\boldsymbol{\theta}$, where $\mathbf{J}_\theta = \partial f(\mathbf{q},\boldsymbol{\theta}) / \partial\boldsymbol{\theta}$ is the kinematic Jacobians with respect to the virtual variables $\boldsymbol{\theta}$, which may be computed from (2) analytically or semi-analytically, using the factorization technique proposed in [12]. On the other hand, for the internal forces $\boldsymbol{\tau}_\theta$, the virtual work includes only one component $-\boldsymbol{\tau}_\theta^{\mathrm{T}} \cdot \Delta\boldsymbol{\theta}$. Therefore, since in the static equilibrium the total virtual work is equal to zero for any virtual displacement, the equilibrium conditions may be written as

$$\mathbf{J}_\theta^{\mathrm{T}} \cdot \mathbf{W} = \boldsymbol{\tau}_\theta \tag{3}$$

This gives additional expressions describing the force/torque propagation from the joints to the end-effector that should be considered simultaneously with the geometric equation (2).

Combining further the virtual joint reaction equation $\boldsymbol{\tau}_\theta = \mathbf{K}_\theta \cdot \boldsymbol{\theta}$, the equilibrium condition (3) and the linearized geometric model $\Delta\mathbf{t} = \mathbf{J}_\theta \cdot \Delta\boldsymbol{\theta}$, it is possible to write statics equations

$$\mathbf{J}_\theta \cdot \boldsymbol{\theta} = \Delta\mathbf{t}; \qquad \mathbf{W} \cdot \mathbf{J}_\theta^{\mathrm{T}} - \mathbf{K}_\theta \cdot \boldsymbol{\theta} = 0 \tag{4}$$

describing elastostatic properties of the considered manipulator. In these equations, the end-effector displacement $\Delta\mathbf{t}$ is treated as the model input and the external wrench $\mathbf{W}$ is the model output, which corresponds to the representation of the manipulator stiffness matrix in the following form

$$\mathbf{W} = \mathbf{K}_{\mathrm{C}} \cdot \Delta\mathbf{t} \tag{5}$$

where $\mathbf{K}_{\mathrm{C}}$ is the desired Cartesian stiffness matrix of the considered manipulator for given robot configuration $\mathbf{q}$. To find this matrix, equations (4) may be presented in the matrix form

$$\begin{bmatrix} \mathbf{0} & \mathbf{J}_\theta \\ \mathbf{J}_\theta^{\mathrm{T}} & -\mathbf{K}_\theta \end{bmatrix} \cdot \begin{bmatrix} \mathbf{W} \\ \boldsymbol{\theta} \end{bmatrix} = \begin{bmatrix} \Delta\mathbf{t} \\ \mathbf{0} \end{bmatrix} \tag{6}$$

and solved for $\mathbf{W}$. This transformation yields the following force-deflection relation $\mathbf{J}_\theta \cdot \mathbf{K}_\theta^{-1} \cdot \mathbf{J}_\theta^{\mathrm{T}} \cdot \mathbf{W} = \Delta\mathbf{t}$ that allows us to express the manipulator Cartesian stiffness matrix as

$$\mathbf{K}_{\mathrm{C}} = \left(\mathbf{J}_\theta \cdot \mathbf{K}_\theta^{-1} \cdot \mathbf{J}_\theta^{\mathrm{T}}\right)^{-1} \tag{7}$$

This expression allows us to compute the Cartesian stiffness matrix assuming that the matrix $\mathbf{K}_\theta = diag(\mathbf{K}_\theta^1,\, \mathbf{K}_\theta^2,\, ...)$, defining elastostatic properties of the manipulator links/joins is given. However, in practice, the matrices $\left\{\mathbf{K}_\theta^{(i)}, i = 1, 2, ...\right\}$ are unknown and should be identified from relevant experiments. However, there are a number of numerical problems that may arise here that are in the focus of the remaining parts of the paper.

## 3. PROBLEM OF ELASTOSTATIC PARAMETERS IDENTIFICATION

### 3.1 Methodology of elastostatic identification

To estimate the desired matrices describing elasticity of the manipulator components (i.e., compliances of the virtual springs presented in Fig. 1), the elastostatic model (5) should be rewritten as

$$\Delta\mathbf{t} = \sum\nolimits_{i=1}^{n} \left(\mathbf{J}_\theta^{(i)} \mathbf{k}_\theta^{(i)} \mathbf{J}_\theta^{(i)\mathrm{T}}\right) \cdot \mathbf{W} \tag{8}$$

where $\Delta\mathbf{t}$ is the vector of the end-effector displacements under the loading $\mathbf{W}$, the matrices $\mathbf{k}_\theta^{(i)} = (\mathbf{K}_\theta^{(i)})^{-1}$ denote the link/joint compliances that should be identified via calibration, and the matrices $\mathbf{J}_\theta^{(i)}$ are corresponding sub-Jacobians obtained by the fractioning of the aggregated Jacobian $\mathbf{J}_\theta^T = [\mathbf{J}_\theta^{(1)^T}, \mathbf{J}_\theta^{(2)^T}, ...]$. For the identification purposes, this expression should be transformed into more convenient form, where all desired parameters (elements of the matrices $\mathbf{k}_\theta^{(i)}, i = 1, 2, ...$) are collected in a single vector $\boldsymbol{\pi} = (k_{\theta 11}^{(1)}, k_{\theta 12}^{(1)}, ... k_{\theta 66}^{(n)})$. It yields the following linear equation

$$\Delta\mathbf{t} = \mathbf{A}_\pi(\mathbf{q}, \mathbf{W}) \cdot \boldsymbol{\pi} \tag{9}$$

where $\mathbf{A}_\pi(.)$ is so-called observation matrix that defines the mapping between the unknown compliances $\boldsymbol{\pi}$ and the end-effector displacements $\Delta\mathbf{t}$ under the loading $\mathbf{W}$ for the manipulator configuration $\mathbf{q}$.

Taking into account that the calibration experiments are carried out for several manipulator configurations defined by the actuated joint coordinates $\mathbf{q}_j,\, j = \overline{1, m}$, the system of basic equations for the identification can be presented in the following form

$$\Delta\mathbf{t}_j = \mathbf{A}_{\pi j}(\mathbf{q}_j, \mathbf{W}_j) \cdot \boldsymbol{\pi} + \boldsymbol{\varepsilon}_j; \qquad j = \overline{1, m} \tag{10}$$

where $\boldsymbol{\varepsilon}_j$ denotes the vector of measurement errors. Further, using these notations and assigning proper weights for each equation, the identification can be reduced to the following optimization problem

$$F = \sum\nolimits_{j=1}^{m} (\mathbf{A}_{\pi j}\boldsymbol{\pi} - \Delta\mathbf{t}_j)^T \boldsymbol{\eta}^T \boldsymbol{\eta} (\mathbf{A}_{\pi j}\boldsymbol{\pi} - \Delta\mathbf{t}_j) \to \min_{\boldsymbol{\pi}} \tag{11}$$

where $\boldsymbol{\eta}$ is the matrix of weighting coefficients that normalizes the measurement data. This minimization problem yields the following solution

$$\hat{\boldsymbol{\pi}} = \left(\sum\nolimits_{j=1}^{m} \mathbf{A}_{\pi j}^T \boldsymbol{\eta}^T \boldsymbol{\eta} \mathbf{A}_{\pi j}\right)^{-1} \cdot \left(\sum\nolimits_{j=1}^{m} \mathbf{A}_{\pi j}^T \boldsymbol{\eta}^T \boldsymbol{\eta} \Delta\mathbf{t}_{\pi j}\right). \tag{12}$$

If the measurement noise is Gaussian (as it is assumed in conventional calibration techniques), expression (12) provides us with a unbiased estimates for which $E(\hat{\boldsymbol{\pi}}) = \boldsymbol{\pi}$. Corresponding covariance matrix evaluating the dispersion of the parameter estimate $\hat{\boldsymbol{\pi}}$ from one identification session to another can be computed as follows

$$\begin{aligned} \mathrm{cov}(\hat{\boldsymbol{\pi}}) = \left(\sum\nolimits_{j=1}^{m} \mathbf{A}_{\pi j}^T \boldsymbol{\eta}^T \boldsymbol{\eta} \mathbf{A}_{\pi j}\right)^{-1} \sum\nolimits_{j=1}^{m} \mathbf{A}_{\pi j}^T \boldsymbol{\eta}^T \boldsymbol{\eta} \boldsymbol{\Sigma}^2 \boldsymbol{\eta}^T \boldsymbol{\eta} \mathbf{A}_{\pi j} \times \\ \times \left(\sum\nolimits_{j=1}^{m} \mathbf{A}_{\pi j}^T \boldsymbol{\eta}^T \boldsymbol{\eta} \mathbf{A}_{\pi j}\right)^{-1} \end{aligned} \tag{13}$$

where the matrix $\boldsymbol{\Sigma}^2 = E(\boldsymbol{\varepsilon} \cdot \boldsymbol{\varepsilon}^T)$ describes the statistical properties of the measurement errors.

It can be proved [18] that the best results in terms of the identification accuracy are achieved if $\boldsymbol{\eta} = \boldsymbol{\Sigma}^{-1}$. It leads to the following covariance matrix of the manipulator compliance parameters

$$\mathrm{cov}(\hat{\boldsymbol{\pi}}) = \left(\sum\nolimits_{j=1}^{m} \mathbf{A}_{\pi j}^T \boldsymbol{\Sigma}^{-T} \boldsymbol{\Sigma}^{-1} \mathbf{A}_{\pi j}\right)^{-1} \tag{14}$$

Such assignment of the weighing coefficients $\boldsymbol{\eta}$ also allows us to avoid the problem of different units in the objective function (11), which arises in straightforward application of the leas-square technique to the robot parameters identification if the measurement system provides both position and orientation data. It should be noted that this particularity is usually omitted in conventional robot calibration. Another way to improve the identification accuracy is related to the proper selection of manipulator measurement configurations $\{\mathbf{q}_j, j = \overline{1,m}\}$ that is also known as the calibration experiment planning [19], which directly influences on the observation matrices $\mathbf{A}_{\pi j}(\mathbf{q}_j, \mathbf{W}_j)$ and on the covariance matrix (14).

It is clear that expression (12) gives reliable estimates of the parameters $\boldsymbol{\pi}$ if and only if the matrix $\sum\nolimits_{j=1}^{m} \mathbf{A}_{\pi j}^T \boldsymbol{\Sigma}^{-T} \boldsymbol{\Sigma}^{-1} \mathbf{A}_{\pi j}$ is invertible. It leads to the problem of the parameter *identifiability* that have been studied by a number of authors for the problem of geometrical calibration [15-16]. Relevant techniques are based on the *information matrix rank analysis* (via either SVD- or QR-decomposition). However, in real industrial practice where the measurement not is non-negligible, the identifiable parameters are not equivalent in terms of accuracy (both absolute and relative) and expression (12) can give rather surprising results for some of them. This motivates revision of the above mentioned notion (parameter identifiability) and its extension taking into account the identification accuracy defined by the *covariance matrix* (14). In the following sub-sections, the notion of *practical identifiability* is introduced and a motivation example is presented, which illustrates potential problems that may arises in the manipulator elastostatic calibrations if conventional techniques are applied.

## 3.2 Motivation example

To illustrate the problems that may arise in identification of the manipulator elastostatic parameters, let us consider a numerical example that deals with a single link of the Orthoglide manipulator (Fig. 2). Its compliance matrix has been obtained in [12] and is equal to

$$\mathbf{k} = \left[\begin{array}{ccc:ccc} 4.50{\cdot}10^{-8} & 0 & 0 & 0 & 0 & 0 \\ 0 & 8.01{\cdot}10^{-5} & 0 & 0 & 0 & 3.98{\cdot}10^{-4} \\ 0 & 0 & 3.64{\cdot}10^{-5} & 0 & -1.71{\cdot}10^{-4} & 0 \\ \hdashline 0 & 0 & 0 & 3.76{\cdot}10^{-3} & 0 & 0 \\ 0 & 0 & -1.71{\cdot}10^{-4} & 0 & 1.09{\cdot}10^{-3} & 0 \\ 0 & 3.98{\cdot}10^{-4} & 0 & 0 & 0 & 2.65{\cdot}10^{-3} \end{array}\right] \tag{15}$$

where the values are expressed in SI units (N, m, rad).

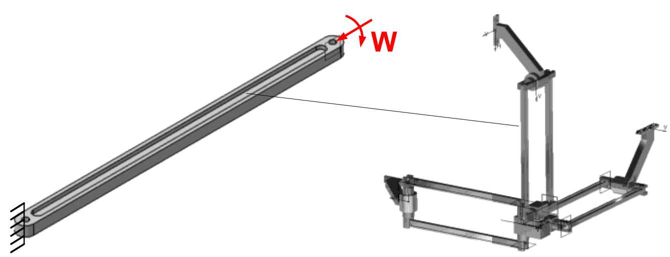


(a) Principal link of Orthoglide manipulator (b) Architecture of Orthoglide manipulator

**Figure 2** Manipulator link considered in the motivation example

Let us simulate the calibration process assuming that the matrix (15) should be estimated by means of the identification algorithm described above, where the input data are generated by means of virtual experiments. In the frame of these experiments, the link is assumed to be fixed on one side and the external loading $\mathbf{W}_j$ is applied on the another side. For each loading, the corresponding deflection vector is computed in accordance with expression $\Delta\mathbf{t}_j = \mathbf{k}{\cdot}\mathbf{W}_j + \boldsymbol{\varepsilon}_j$, where $\boldsymbol{\varepsilon}_j$ is the measurement noise. In accordance with the physical properties of the examined link and to conserve the linearity of the force-deflection relation, the loading magnitude has been limited by $10N$ for the forces and $10Nm$ for the torques. The measurement noise magnitude has been defined as $\sigma_p = 25\mu m$

 

for the positional components and as $\sigma_\varphi = 0.25\,mrad$ for the orientation components (these values correspond to the precision of the best industrial measurement systems that currently are available on the market). These virtual experiments has been carried out six times, in order to obtain sufficient number of equations for the identification of 36 desired parameters $k_{ij}$.

For these virtual experiments, the properties of the observation matrix used in the identification expression are quite good: rank is equal to 36 and the condition number is 1.00. Nevertheless, the identification are rather "surprising": the obtained compliance matrix essentially differs from the original one and is

$$\hat{\mathbf{k}} = \left[\begin{array}{ccc:ccc} -3.05\cdot10^{-8} & -8.71\cdot10^{-8} & 1.86\cdot10^{-7} & 1.59\cdot10^{-7} & -7.72\cdot10^{-8} & 1.15\cdot10^{-7} \\ 4.53\cdot10^{-7} & 8.05\cdot10^{-5} & -2.07\cdot10^{-7} & 1.98\cdot10^{-7} & 1.14\cdot10^{-7} & 3.98\cdot10^{-4} \\ 2.29\cdot10^{-7} & 3.76\cdot10^{-7} & 3.65\cdot10^{-5} & -2.25\cdot10^{-7} & -1.71\cdot10^{-4} & 1.13\cdot10^{-7} \\ \hdashline -1.42\cdot10^{-7} & 1.83\cdot10^{-6} & 7.05\cdot10^{-7} & 3.76\cdot10^{-3} & 1.11\cdot10^{-6} & 4.12\cdot10^{-6} \\ 3.27\cdot10^{-6} & 1.23\cdot10^{-6} & -1.68\cdot10^{-4} & 3.99\cdot10^{-6} & 1.09\cdot10^{-3} & -5.07\cdot10^{-6} \\ -2.61\cdot10^{-6} & 3.97\cdot10^{-4} & -1.06\cdot10^{-6} & 2.81\cdot10^{-7} & -4.58\cdot10^{-8} & 2.65\cdot10^{-3} \end{array}\right] \quad (16)$$

Detailed comparison analysis of the original matrix $\mathbf{k}$ and its estimate $\hat{\mathbf{k}}$ allows us to make the following conclusions concerning the harmful impact of the measurement noise on the identification of the elastostatic parameters in real industrial environment:

(i) the obtained compliance matrix $\hat{\mathbf{k}}$ *may lose the properties of positive-definiteness*, which completely contradicts to the common physical sense that is based on the energy-based definition of $\mathbf{k}^{-1}$ (in particular, in the above example, $\hat{\mathbf{k}}_{11} < 0$ is not acceptable);

(ii) the obtained matrix $\hat{\mathbf{k}}$ *may be non-symmetric*, which also contradicts to the physical sense (for instance, $\hat{\mathbf{k}}_{53}$ and $\hat{\mathbf{k}}_{35}$, which corresponds to non-zero elements of $\mathbf{k}$, are not equal and differ by 2%);

(iii) for some small elements, the *identification accuracy may be extremely low* (for example the element $\hat{\mathbf{k}}_{11}$, which is $\sim 10^3$ times less than $\hat{\mathbf{k}}_{22}$ and $\hat{\mathbf{k}}_{33}$ has been identified completely wrongly);

(iv) in the obtained matrix $\hat{\mathbf{k}}$, the *number of non-zero elements is redundant* compared to the original matrix $\mathbf{k}$; moreover, it is difficult to distinguish small elements $\hat{k}_{ij}$ from so-called zero elements, which correspond to exact zeros in $\mathbf{k}$ induced by the physical properties of the examined link (for instance, the element $\hat{k}_{21}$ that should be equal to zero by definition is the same order of magnitude as $\hat{k}_{11}$, which should be small but strictly positive);

(v) *for the remaining elements*, whose magnitude is high enough, the *identification errors are quite acceptable* (from 0.01% to 1.67%), but they should be further reduced by increasing number of the experiments.

It should be noted that for essentially lower measurement noise (with $\sigma_p$ and $\sigma_\varphi$ that are 100 times smaller) the above mentioned problems do not exist, however such measurement precision is not achievable in industrial environment at present.

Hence, as follows from this motivation example, the whole set of 36 elastostatic parameters $\{k_{ij}\}$ composing the $6\times6$ matrix $\mathbf{k}$ cannot be estimated using commercially available measurement systems. The main reason for this difficulty is that, for some elements, corresponding deflections under the admissible loading are comparable with the measurement noise. To detect these indistinct elements, a simple indicator can be applied showing *parameter-to-noise ratio* (which is similar to signal-to-noise ratio in communication):

$$\left[\frac{|\hat{k}_{ij}|}{\sigma_{ij}}\right] = \left[\begin{array}{ccc:ccc} 0.12 & 0.35 & 0.74 & 0.64 & 0.31 & 0.46 \\ 1.81 & 322 & 0.83 & 0.79 & 0.46 & 1593 \\ 0.91 & 1.50 & 146 & 0.89 & 684 & 0.45 \\ \hdashline 0.06 & 0.73 & 0.28 & 1504 & 0.44 & 1.64 \\ 1.31 & 0.49 & -67.3 & 1.60 & 436 & 2.02 \\ 1.04 & 159 & 0.42 & 0.11 & 0.02 & 1060 \end{array}\right] \quad (17)$$

where $\sigma_{ij}$ is a corresponding element of the relevant covariance matrix. As follows from these numerical values, 27 of 36 desired parameters can be hardly estimated from the experimental data with realistic measurement noise. Only for 9 parameters $k_{22}$, $k_{26}$, $k_{33}$, $k_{35}$, $k_{44}$, $k_{53}$, $k_{55}$, $k_{62}$, $k_{66}$ the ratio is high enough (more than 50), so they can be treated as "*practically identifiable*". It should be stressed that similar indicators computed using exact values of $k_{ij}$ (which are unknown in practice) give similar result

$$\left[\frac{|k_{ij}|}{\sigma_{ij}}\right] = \left[\begin{array}{ccc:ccc} 0.18 & 0 & 0 & 0 & 0 & 0 \\ 0 & 320 & 0 & 0 & 0 & 1592 \\ 0 & 0 & 146 & 0 & 684 & 0 \\ \hdashline 0 & 0 & 0 & 1504 & 0 & 0 \\ 0 & 0 & 68.4 & 0 & 436 & 0 \\ 0 & 159 & 0 & 0 & 0 & 1060 \end{array}\right] \quad (18)$$

allowing us to detect the same set of small or zero parameters whose identifiability is questionable. On the other side, the impact of these parameters on the elastostatic deflections is so small that they can be reasonably excluded from the desired stiffness model. These results confirm importance of the above pointed problems, which below are considered in details.

### 3.3 Research problem: practical identifiability

Summarizing theoretical background and simulation results presented in previous sub-sections, it is possible to make the following conclusions:

(i) complete elastostatic model of robotic manipulator includes *huge number of parameters* (258 for conventional 6 d.o.f. serial robot), whose simultaneous identification in presence of measurement noise is rather difficult or even impossible;

 

(ii) before applying the least-square identification technique , the manipulator elastostatic model should be reduced and *redundant parameters* should be eliminated, in order to ensure invertibility of the information matrix; this step can be performed using techniques similar to those developed for the geometrical calibration;

(iii) among the remaining non-redundant parameters, there are a number of non-significant ones, whose absolute values are relatively small, the identification accuracy is quite low and the impact on the compliance of the of the entire manipulator is almost negligible; these parameters can be treated as "*practically non-identifiable*" and should be also eliminated from the model, but relevant techniques are not available yet;

(iv) while developing relevant techniques allowing detection of "*practically identifiable*" *parameters*, it is prudent to take into account some specific properties of the compliance matrices induced by the elasticity physics such as the compliance matrix symmetry, presence of strictly zero elements (matrix sparseness), positive-definiteness, etc.

Hence, to obtain reliable stiffness model that is suitable for calibration, contains only significant and practically identifiable parameters while describing manipulator elastostatic properties sufficiently good, it is necessary to develop dedicated model reduction techniques and relevant rules allowing us to minimize number of parameters to be estimated and to reconstruct the original VJM-based model from these data taking into account mathematical relations between the model parameters caused by their physical sense.

## 4. PRACTICAL IDENTIFIABILITY IN MANIPULATOR CALIBRATION

### 4.1 Basic assumptions and terminology

Let us assume that the vector of desired elastostatic parameters $\boldsymbol{\pi}$ should be identified from the set of the linear equations (10) whose least square solution is defined by the expression (12), where the observation matrices $\mathbf{A}_{\pi j}(\mathbf{q}_j, \mathbf{W}_j)$ are computed for certain set of measurement configurations $\{\mathbf{q}_j\}$ and loadings $\mathbf{W}_j$. Depending on the matrix set $\{\mathbf{A}_{\pi j}\}$, corresponding system of linear equations can be solved for $\boldsymbol{\pi}_k$ either uniquely or may have infinite number of solutions. In general, if the information matrix is rank-deficient, a general solution of the system (10) can be presented in the following form

$$\hat{\boldsymbol{\pi}} = \mathbf{A}_\Sigma^+ \cdot \mathbf{B}_\Sigma + \left(\mathbf{I} - \mathbf{A}_\Sigma^+ \mathbf{A}_\Sigma\right) \cdot \boldsymbol{\lambda} \,. \tag{19}$$

where the superscript "+" denotes the Moore–Penrose pseudo inverse, $\mathbf{A}_\Sigma = \sum_{j=1}^m \mathbf{A}_{\pi j}^T \boldsymbol{\eta}^T \boldsymbol{\eta} \mathbf{A}_{\pi j}$ , $\mathbf{B}_\Sigma = \sum_{j=1}^m \mathbf{A}_{\pi j}^T \boldsymbol{\eta}^T \boldsymbol{\eta} \Delta\mathbf{t}_{\pi j}$ and $\boldsymbol{\lambda}$ is an arbitrary vector of the same size as $\boldsymbol{\pi}$ . Using the later expression, all desired parameters contained in the vector $\boldsymbol{\pi}$ can be divided into the following groups [16]:

**G1:** *Identifiable* parameters that can be obtained from (19) in unique way and are independent from the arbitrary vector $\boldsymbol{\lambda}$ ;

**G2:** *Non-identifiable* parameters that cannot be computed uniquely from (19) and can take on any value without influence on the right-hand side of the equation (9), they correspond to the zero columns of the observation matrix $\mathbf{A}_\pi$ ;

**G3:** *Semi-identifiable* parameters that are also cannot be computed uniquely but have influence on the right-hand side of the equation (9); they are united in subgroups where a single one can be treated as identifiable if the remaining ones are fixed.

To obtain typical examples of the parameters belonging to the groups G1, G2 and G3, it is possible to use the ideas similar to geometrical calibration. For instance, the elastostatic parameters of the actuated joints and adjacent links are redundant in their totality and belong to the group G3. Besides, if the loading direction cannot be altered, a number of parameters belong to the group G2 and cannot be identified from the corresponding experimental data.

In this paper, in contrast to previous works, this classification is enhanced taking into account practical issues related to the limited precision of the measurement system. The main idea is to compare the absolute value of the estimated parameter with the range of possible fluctuations of the estimate caused by the measurement noise. For computational reasons, it is convenient to introduce a numerical indicator similar to the signal-to-noise ratio in communication, which is defined as follows

$$\nu_i = \left|\hat{\pi}_i\right| / \sigma_i, \quad i = 1, 2, ... \tag{20}$$

where $\sigma_i$ is the standard deviation of the parameter estimate $\hat{\pi}_i$ extracted from the diagonal of the covariance matrix (14). It is clear that $\nu_i$ can be treated as the inverse of the relative accuracy, which allows us to avoid the problem of division by zero. In the following sections this indicator will be referred to as *parameter-to-noise ratio*.

Using the above defined indicator, the set of parameters belonging to the group G1 (theoretically identifiable) can be further divided into three subgroups:

**G1+:** *Practically identifiable parameters*, for which the accuracy indicator is high: $\nu_i > \nu_0^+$; this subgroup describes principal elastostatic properties of the manipulator and should be certainly included in the reduced model used in the identification routines;

**G1-:** *Practically non-identifiable parameters*, for which the accuracy indicator is low: $\nu_i < \nu_0^-$; this subgroup contains non-essential parameters that can be assigned to zero in the VJM-model without essential impact on its precision (in practice, the majority of these parameters are nominally equal to zero due to the physical nature of the compliance matrices);

**G1~:** *Practically semi-identifiable parameters*, for which the accuracy indicator is intermediate: $\nu_0^- \le \nu_i \le \nu_0^+$; the parameters belonging to this subgroup are practically non-identifiable for the current experimental setup but, hypothetically, can be converted into practically identifiable ones by increasing the experiment number, improving the measurement precision of by modification of the measurement configurations.

An open question however is related to justified assigning of the upper and lower bounds $\nu_0^+$ and $\nu_0^-$. From practical point of view that is adopted below, it is reasonable to use $\nu_0^+ = 5$ and $\nu_0^- = 2$, which is in a good agreement with the quantiles of the normal distribution. However, the user may modify these values in accordance with the specificity of the problem of interest.

The above presented definitions allow us to revise the concept of "*suitable-for-calibration*" model that in previous works included all parameters of the group G1 (this model is also referred to as the "complete and irreducible" one). In this work, this model is limited to include only parameters of the subgroup G1+ (practically identifiable) that can be estimated with reasonable accuracy and provide good approximation of the original complete model. The following subsections address different aspects of model reduction allowing us to obtain the desired model suitable for the elastostatic calibration.

It should be noted that, in spite of the fact that the main focus of the paper is on the elastostatic modelling, similar ideas can be also successfully applied in manipulator geometric calibration.

### 4.2 Model reduction: physical approach

Straightforward approach to the manipulator stiffness modeling leads to the exhaustive but redundant number of parameters to be identified. For instance, each links is described by a $6\times6$ matrix that includes 36 parameters that are treated as independent ones. However, as follows from physics, number of the pure physical and independent parameters is essentially lower (for a trivial prismatic beam, for example, there are only five physical parameters: three describing the geometry and two describing the material properties). Hence, there are strong relations between these 36 parameters but this fact is usually ignored in elastostatic calibration. Besides, due to fundamental properties of conservative system, the desired compliance matrices should be strictly symmetrical and positive-definite. In addition, for typical manipulator links, the compliance matrices are sparsed due to the shape symmetry with respect to some axis, but this property is also not taken into account in identification of the elastostatic parameters.

To take advantages of the compliance matrix properties and to increase the identification accuracy, two simple methods can be applied that allows us to reduce the number of parameters to be computed in the identification procedure (12). They can be treated as the physics-based model reduction techniques and formalized in the following way.

**M1**:**Symmetrisation.** For all compliance matrices $\mathbf{k}$ to be identified, replace the pairs of symmetrical parameters $\{k_{ij}, k_{ji}\}$ by a single one $k_{ij}$, $i<j$.

For each link, this reduction procedure is equivalent to re-definition of the model parameters vector in the following way

$$\boldsymbol{\pi} = \mathbf{M}\cdot\boldsymbol{\pi}' \tag{21}$$

where the binary matrix $\mathbf{M}$ of size $36\times21$ describes the mapping from the original to reduced parameter space. It can be proved that corresponding basic expression for the identification (9) can be rewritten as

$$\Delta\mathbf{t} = \mathbf{A}'_\pi(\mathbf{q},\mathbf{W})\cdot\boldsymbol{\pi}' \tag{22}$$

where $\mathbf{A}'_\pi(.) = \mathbf{A}_\pi(.)\cdot\mathbf{M}$ denotes the reduced observation matrix. The later can be also computed as

$$\mathbf{A}'_\pi(\mathbf{q},\mathbf{W}) = [\mathbf{J}_\theta\boldsymbol{\omega}_1\mathbf{J}_\theta^T\mathbf{W},\ \mathbf{J}_\theta\boldsymbol{\omega}_2\mathbf{J}_\theta^T\mathbf{W},\ ...\mathbf{J}_\theta\boldsymbol{\omega}_{21}\mathbf{J}_\theta^T\mathbf{W}] \tag{23}$$

where $\boldsymbol{\omega}_1, \boldsymbol{\omega}_2, ...$ denote the binary matrices of size $6\times6$ for which non-zero elements (i.e. equal to 1) are located in the following way: for the parameter $\pi_l$ corresponding to the matrix elements $k_{ij}$, $i\le j$, the non-zero elements are $\omega_{ij} = \omega_{ji} = 1$. It is clear that this idea allows us to reduce the number of links compliance parameters from 36 to 21 (and from 258 to 153 for the entire 6 d.o.f. manipulator).

**M2**:**Sparcing.** For all compliance matrices $\mathbf{k}$ to be identified, eliminate from the set of unknowns the parameters $k_{ij}$ corresponding to zeros in the stiffness matrix template $\mathbf{k}^0$ derived analytically for the manipulator link with similar shape.

To derive the desired template matrix it is convenient to use any realistic link-shape approximation. For example using the trivial beam [20], the desired template can be presented as

$$\mathbf{k}^0 = \left[\begin{array}{ccc:ccc} * & 0 & 0 & 0 & 0 & 0 \\ 0 & * & 0 & 0 & 0 & * \\ 0 & 0 & * & 0 & * & 0 \\ \hdashline 0 & 0 & 0 & * & 0 & 0 \\ 0 & 0 & * & 0 & * & 0 \\ 0 & * & 0 & 0 & 0 & * \end{array}\right] \tag{24}$$

where the symbol "*" denotes non-zero elements. It allows further reducing the number of the unknown parameters from 21 to 8, taking into account only essential ones from physical point of view. It can be also proved that the template (24) is valid for any link whose geometrical shape is symmetrical with respect to three orthogonal axes. But it is necessary to be careful if this property is not kept strictly.

Summarizing these methods, it should be mentioned that the above presented methods essentially reduce the number of parameters to be identified (by the factor 4.5) but they do not violate such basic properties as the mode completeness, i.e. the ability to describe any deflection caused by the external loading. However, the reduced model may still have some redundancy in the frame of entire manipulator, where the virtual springs of adjacent joints/actuators cause similar impact on the end-effector deflections under the loading. To eliminate these parameters (belonging to the group G3), relevant algebraic technique developed in our previous work [16] can be applied.

To illustrate efficiency of the proposed methods, the identification problem considered in section 3.2 have been solved for reduced set of the compliance parameters. It yielded the following result

$$\hat{\mathbf{k}} = \left[\begin{array}{ccc:ccc} -3.05\cdot10^{-8} & 0 & 0 & 0 & 0 & 0 \\ 0 & 8.05\cdot10^{-5} & 0 & 0 & 0 & 3.98\cdot10^{-4} \\ 0 & 0 & 3.64\cdot10^{-5} & 0 & -1.71\cdot10^{-4} & 0 \\ \hdashline 0 & 0 & 0 & 3.76\cdot10^{-3} & 0 & 0 \\ 0 & 0 & -1.71\cdot10^{-4} & 0 & 1.09\cdot10^{-3} & 0 \\ 0 & 3.98\cdot10^{-4} & 0 & 0 & 0 & 2.65\cdot10^{-3} \end{array}\right] \tag{25}$$

which is essentially better compared to (16). In particular, the identification errors for the most of the desired parameters are less than 0.4%, i.e. 4 times lower. The only exception is the small element $\hat{k}_{11}$ that is still negative and contradicts to the physical sense. This motivates further efforts to obtain reliable model suitable for elastostatic calibration in industrial environment.

## 4.3 Model reduction: statistical approach

As follows from relevant study and above presented example, rigorous reduction methods based on the physical and mathematical properties of the compliance matrix are rather limited if the measurement noise is non- negligible. This gives us reasons to develop some heuristic rules that take into account the measurement noise impact on the identification accuracy. It is clear that extremely low accuracy is not acceptable, but often corresponding parameters are so small that their influence on the end-effector deflections is almost negligible. This supports an idea for heuristic reduction of small model parameters but leaving an open problem of their further reconstruction in the VJM-model using some empirical or semi-empirical relations induced by mathematical relations between the stiffness matrix elements.

To take into account the relative accuracy of the parameter estimates, it is convenient to use a simple indicator showing parameter-to-noise ratio (20) introduced in sib-section 4.1. It is evident that it should be applied only to those parameters that belong to the group G1 (theoretically identifiable). Using this index, a heuristic model reduction technique allowing us to distinguish the practically identifiable parameters from the hardly-identifiable ones can be formalized as follows:

**M3**:**Neglecting.**

*Step* 1: Using complete but non-redundant model derived after application of physical and algebraic model reduction techniques, compute estimates of the desired parameters $\hat{\boldsymbol{\pi}}'$ and their covariance matrix $\operatorname{cov}(\hat{\boldsymbol{\pi}}')$ by means of equations (12) and (14);

*Step* 2: Using the parameters estimates $\hat{\boldsymbol{\pi}}'$ and the diagonal elements of the covariance matrix $\operatorname{cov}(\hat{\boldsymbol{\pi}}')$, compute the parameter-to-noise ratios $\nu_i$ in accordance with expression (20);

*Step* 3. For all compliance matrices $\mathbf{k}$ to be identified, eliminate from the set of unknowns the parameters $k_{ij}$ for which parameter-to-noise ratios $\nu_{ij}$ is lower the user defined threshold: $\nu_{ij} < \nu_0^+$.

This method allows us to eliminate from the model the parameters whose identification accuracy is comparable with the noise impact and, strictly speaking, these values can not be considered as reliable estimates of $k_{ij}$.

As follows from our experience, it a very powerful method with two useful features: (i) elimination of small (but theoretically non-zero) parameters, and (ii) detection of elements corresponding to zeros in the matrix template (see method M2), if the latter has been defined rather carefully. These conclusions are clearly confirmed by the numerical example presented in section 3.2 (see (17) and (18)). In this example, it is worth to pay attention to the element $\hat{k}_{11}$ that is really small for the majority of manipulator links (because the link length is always essentially higher compared to the cross-section dimensions). Elimination of this parameter is really negligible for the manipulator Cartesian stiffness matrix (7) that integrates impact of all compliance elements. Nevertheless, after identification, the parameter $\hat{k}_{11}$ can be reconstructed approximately using non-zero elements of the compliance matrix and some relations between $\hat{k}_{ij}$ induced by physics. The last problem is currently under study but is not in the scope of this paper.

In conclusion of this section, it should be noted that the proposed methods M1-M3 allow us essentially reducing the number of model parameters while retaining the model accuracy. For example, for 6 d.o.f. manipulator, the number of parameters is reduced from 258 to 42 allowing us to obtain an adequate stiffness model in real industrial environment.

## 5. APPLICATION EXAMPLE

The developed model reduction techniques have been applied to the elastostatic identification of the industrial robot KUKA KR-270 (Figure 3), which is used for processing of aircraft components made from contemporary high performance materials. The application area requires high positional precision while the technological process generates significant end-effector deflections, which can be compensated on the control level via the elastostatic modeling. It should be noted that for this robot, the elastostatic model must also take into account the impact of the gravity compensator, which creates the closed loop between the first and second links and is described in the stiffness model by two additional parameters (the spring stiffness and preloading). The geometrical parameters of the gravity compensator have been identified from dedicated experiments.


**Figure 3** Experimental setup for the identification of the elastostatic parameters

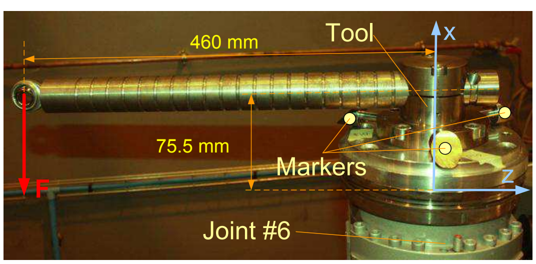


**Figure 4** End-effector used for elastostatic calibration experiments

For the elastostatic calibration, two different experiment setups have been used. The first of them is based on the application of the gravity force 2.5 kN to the special measurement tool, which contains three reference points (Figure 4). Relevant deflections have been measured by the laser-tracer Leica (absolute accuracy 10μm). For the second setup, the deflections have been generated by applying horizontal loadings 3.5 kN. To find the measurement configurations that ensure the best identification accuracy, the design of experiments technique has been applied, which is based on the dedicated industry-oriented performance measure proposed in our previous work [16]. These optimal configurations have been obtained taking into account physical constraints that are related to the joint limits and the work-cell obstacles.

**Table 1** Principal elastostatic parameters of KR-270

| Parameter | Value | Accuracy |
|---|---|---|
| $k_c$, [rad·μm/N] | 0.144 ±0.031 | 21.5% |
| $s_0$, [mm] | 458 ±27 | 5.9% |
| $k_2$, [rad·μm/N] | 0.302 ± .004 | 1.3% |
| $k_3$, [rad·μm/N] | 0.406 ±0.008 | 2.0% |
| $k_4$, [rad·μm/N] | 3.002 ±0.115 | 3.8% |
| $k_5$, [rad·μm/N] | 3.303 ±0.162 | 4.9% |
| $k_6$, [rad·μm/N] | 2.365 ±0.095 | 4.0% |

For the considered manipulator, the complete elastostatic model includes 260 parameters (with 2 additional parameters for the gravity compensator). To obtain the suitable for calibration model, the original set of parameters has been sequentially reduced by applied physical, algebraic and statistical methods presented in Section 4. This yielded the simplified model with 18 parameters that can be identified in practice with the desired accuracy (the most essential of them corresponding to the joint actuators are presented in Table 1). Relevant model has been further used for the compliance error compensation for the robotic based milling of a aircraft parts, where essential improvement of the precision has been achieved. For this application, the reduced elastostatic model allowed us to compensate more than 95% of elastostatic deflections and to ensure positional accuracy about 0.1 mm (that is comparable with the robot repeatability 0.06 mm).

## 6. CONCLUSIONS

The paper deals with the problem of the manipulator stiffness modeling, which is extremely important for the robotic-based machining of contemporary aeronautic materials where high position accuracy is required while performing prescribed manufacturing task. The main attention is paid to the elastostatic parameters identification and model reduction, where the notion of practical identifiability is introduced that relies on the essential differences in the model parameter magnitudes and the measurement noise impact.

In contrast to previous works, the manipulator stiffness properties are described by the sophisticated model, which takes into account the flexibilities of all mechanical elements such as links, actuated joints, mechanical transmissions, etc.. In the frame of this model, the virtual joint method (VJM) is used, which operates with 6×6 stiffness matrices for each compliant link and scalar coefficients for the joints/transmissions. This yields extremely high number of the model elastostatic parameters to be identified, that for a conventional 6 d.o.f. manipulator reaches 258. Even by eliminating dependent ones does not allow us to reduce this number substantially; for this manipulator the stiffness model includes 153 independent parameters that, theoretically, may be identified. However, the parameter magnitudes differ significantly (~1000 times), so straightforward application of conventional identification technique does not give reliable results (for some parameters the estimation errors are greater than 100% that also may violate fundamental physical properties of the stiffness matrices, such as *positive-definiteness and symmetry*). On the other hand, some of the desired parameters are so small that their influence on the manipulator accuracy is negligible. This leads the problem of further reduction of the stiffness model that aims at eliminating some small parameters. To distinguish these small parameters from essential ones, the notion of practical identifiability is introduced.

To solve the problem, physical and statistical model reduction methods are developed. They take into account mathematical relations between the elements of the compliance matrices and parameter magnitude with respect to the measurement noise impact. The advantages of the developed approach are illustrated by an application example that deals with the stiffness modeling of industrial robot used in aerospace industry. In future, the problem of the complete model reconstruction from the obtained set of practically identifiable parameters will be in the focus of our attention.

## ACKNOWLEDGMENTS

The work presented in this paper was partially funded by the Region “Pays de la Loire”, France and by the projects ANR COROUSSO and FEDER ROBOTEX, France.

## REFERENCES

[1] Dépincé, P., Hascoët, J-Y., 2006, "Active integration of tool deflection effects in end milling. Part 2. Compensation of tool deflection," International Journal of Machine Tools and Manufacture, vol. 46, pp. 945-956

[2] Kövecses, J., Angeles, J., 2007, "The stiffness matrix in elastically articulated rigid-body systems," Multibody System Dynamics. vol. 18(2), pp. 169–184.

[3] Eastwood, S.J., Webb, P., 2010, "A gravitational deflection compensation strategy for HPKMs," Robotics and Computer-Integrated Manufacturing, vol. 26 pp. 694–702

[4] Klimchik, A., Pashkevich, A., Chablat, D., Hovland G., 2013, "Compliance error compensation technique for parallel robots composed of non-perfect serial chains," Robotics and Computer-Integrated Manufacturing Journal, Vol. 29, Issue 2, pp. 385–393

[5] Chen, Y., Gao, J., Deng, H., Zheng, D., Chen, X., Kelly, R., 2013, "Spatial statistical analysis and compensation of machining errors for complex surfaces," Precision Engineering, Vol. 37, Issue 1, pp. 203-212

[6] Piras, G., Cleghorn, W.L., Mills, J.K., 2005, "Dynamic finite-element analysis of a planar high-speed, high-precision parallel manipulator with flexible links," Mechanism and Machine Theory, vol. 40(7), pp. 849–862.

[7] Long, C.S., Snyman, J.A., Groenwold, A.A., 2003, "Optimal structural design of a planar parallel platform for machining," Applied Mathematical Modelling, vol. 27 (8), pp. 581–609.

[8] Deblaise, D., Hernot, X., Maurine, P., 2006, "A systematic analytical method for PKM stiffness matrix calculation," Proceedings of the IEEE International Conference on Robotics and Automation (ICRA), pp. 4213-4219.

[9] Chen, S., Kao, I., 2000, "Conservative Congruence Transformation for Joint and Cartesian Stiffness Matrices of Robotic Hands and Fingers," The International Journal of Robotics Research, vol. 19(9), pp. 835–847.

[10] Alici, G., Shirinzadeh, B., 2005, "Enhanced stiffness modeling, identification and characterization for robot manipulators," Proceedings of IEEE Transactions on Robotics, vol. 21(4), pp. 554–564.

[11] Quennouelle, C., Gosselin, C.M., 2008, "Stiffness Matrix of Compliant Parallel Mechanisms," Advances in Robot Kinematics: Analysis and Design, pp. 331-341.

[12] Pashkevich, A., Chablat, D., Wenger, Ph., 2010, "Stiffness analysis of overconstrained parallel manipulators," Mechanism and Machine Theory, vol. 44, pp. 966-982.

[13] Pashkevich, A., Klimchik, A., Chablat, D., 2011, "Enhanced stiffness modeling of manipulators with passive joints", Mechanism and Machine Theory, vol. 46(5), pp. 662-679.

[14] Everett, L., M. Driels and B. Mooring, 1987, "Kinematic modelling for robot calibration," Proc. of the IEEE Conf. on Robotics and Automation, p. 183-189.

[15] Khalil, W., Dombre, E., 2004 "Modeling, Identification and Control of Robots," Butterworth-Heinemann, Technology & Engineering - 500 pages

[16] Pashkevich, A., 2001, "Computer-aided generation of complete irreducible models for robotic manipulators," Int. Conference of Modellimg and Simulation., pp. 293-298.

[17] Angeles, J., 2007, "Fundamentals of Robotic Mechanical Systems: Theory, Methods, and Algorithms," Springer, New York.

[18] J.A. Rice (1995). Mathematical Statistics and Data Analysis. Second Edition. Duxbury Press.

[19] Daney, D., Papegay, Y., Madeline, B., 2005, "Choosing measurement poses for robot calibration with the local convergence method and Tabu search." The International Journal of Robotics Research, vol. 24, pp. 501-518.

[20] Timoshenko, S., Goodier, J.N., 1970, "Theory of elasticity," 3d ed., McGraw-Hill, New York

 